Journal of Alloys and Compounds 516 (2012) 107–112

Contents lists available at SciVerse ScienceDirect

Journal of Alloys and Compounds

journal homepage: www.elsevier.com/locate/jallcom

Subsolidus phase relations in $CaO–In_2O_3–B_2O_3$ system and crystal structure of $CaInBO_4$

H.K. Li [a,b], G.M. Cai [a,b,*], J.J. Fan [a,b], Z.P. Jin [a,b]

[a] Science Center for Phase Diagram & Materials Design and Manufacture, Central South University, Changsha, Hunan 410083, PR China
[b] School of Materials Science and Engineering, Central South University, Changsha, Hunan 410083, PR China

ARTICLE INFO

Article history:
Received 21 September 2011
Received in revised form
19 November 2011
Accepted 29 November 2011
Available online 8 December 2011

Keywords:
Calcium indium borate
Solid state reactions
Crystal structure
X-ray diffraction

ABSTRACT

Subsolidus phase relations of $CaO–In_2O_3–B_2O_3$ system have been investigated mainly by the conventional solid-state reaction technique and powder X-ray diffraction method. There are nine definite three-phase regions under present experimental conditions. Six binary compounds and one ternary compound were found to exist in this system. Crystal structure of the ternary compound $CaInBO_4$ was determined from X-ray powder diffraction data using Rietveld method. It crystallizes in the orthorhombic space group Pnma (No. 62) with $a = 10.3120(3)$ Å, $b = 3.42519(8)$ Å, $c = 9.5150(3)$ Å, $V = 336.07(2)$ Å^3 and $Z = 4$. Mixed occupancies were confirmed in this structure, Ca and In atoms are distributed between two atom sites: 93.6%Ca and 6.4%In occupy one site, 93.6%In and 6.4%Ca occupy another. Two $In(Ca)O_6$ octahedra and two $Ca(In)O_7$ polyhedra are linked each other by sharing edges to form ribbons in the *a*–*c* plane and extend infinitely along the direction of the *b* axis. The infrared spectrum of $CaInBO_4$ has been measured, which is consistent with the crystallographic study. In general, compounds $MRBO_4$ (M and R are divalent and trivalent cations, respectively) are in a large family of monoborates with different structure types strictly depending on the relative size of the M and R ions.

1. Introduction

Over a long period of time, borates have been established as useful functional materials with rich crystal structure [1–3], wide transparency spectra range, and large band gap. The trivalent-metal or rare-earth-metal borates have been given intense attention because of their outstanding optical properties, for instance, $K_2Al_2B_2O_7$ (KAB) [4] for second harmonic generation or YBO_3, $Li_6GdB_3O_9$ and $Ba_3InB_9O_{18}$ for host of phosphor [5–7]. Our group have made systematic surveys on the $MO–R_2O_3–B_2O_3$ (M = alkaline-earth metal, R = Sc, In, rare-earth metal) systems to search for new functional materials. Very recently, we investigated subsolidus phase relations in $CaO–In_2O_3–B_2O_3$ system based on exploratory syntheses via solid-state reactions, which led to the discovery of the ternary compound $CaInBO_4$. Blasse [8] and Capponi et al. [9] have ever reported the lattice parameters of $CaInBO_4$. However, the crystal structure of $CaInBO_4$ was not reported until now. In this work, the crystal structure of $CaInBO_4$ was investigated and determined by Rietveld method, with structure $CaYBO_4$ as a reference [10]. In addition, structure types of compounds $MRBO_4$ (M = divalent cations; R = trivalent cations) were reviewed in this paper.

2. Experiment

Samples were synthesized by high temperature solid state reactions. Stoichiometric mixtures of $CaCO_3$ (spectral reagent), In_2O_3 (analytical reagent), and H_3BO_3 (analytical reagent) were ground into powders of 200–300 mesh in the agate mortar. The mixtures were preheated in corundum crucibles for 12 h at 600 °C to decompose H_3BO_3 and $CaCO_3$. Then they were cooled, reground and sintered at 800–1350 °C (depending on their compositions) for 24 h. Finally, all the samples were naturally cooled to room temperature. In all cases, special care was taken to add extra 0.2 mol% H_3BO_3 in order to offset the losses of B_2O_3 in the procedure of synthesis.

X-ray powder diffraction (powder XRD) technology, Inorganic Crystal Structure Database (ICSD release 2011) and Powder Diffraction File (PDF release 2009) were used for phase analysis of the samples. The powder XRD patterns were collected on an X-ray Rigaku diffractometer D/MAX-2500 with Cu Kα radiation and graphite monochromator operated at 40 kV, 150 mA. The samples were considered to reach phase equilibrium when their powder XRD patterns showed no change upon successive heat treatments. Data for crystal structure analysis were collected at room temperature in the step-scanning mode with a step size 0.02° (2θ), counting time 2 s per step and 2θ range of 10–130°.

With the samples dissolved in nitric acid at boiling point for 1 h, the atomic ratios of Ca, In, and B for phases were measured by inductively coupled plasma atomic emission spectrometry on a Perkin Elmer ICP/6500 spectrometer.

Infrared (IR) spectroscopy was carried out with the objective of specifying and comparing the coordination of boron in the title compound. The mid-infrared

---

* Corresponding author at: School of Materials Science and Engineering, Central South University, Changsha, Hunan 410083, PR China. Tel.: +86 0731 88877 732.
E-mail addresses: gmcai2002@163.com, caigemei@csu.edu.cn (G.M. Cai).

0925-8388/$ – see front matter © 2011 Elsevier B.V. All rights reserved.
doi:10.1016/j.jallcom.2011.11.145

Table 1
List of phase identification in the system CaO–In_2O_3–B_2O_3.

Samples	CaO (at.%)	$InO_{1.5}$ (at.%)	$BO_{1.5}$ (at.%)	Synthesis temperature	Phase composition
1	20	5	75	800	$CaB_6O_{10} + CaB_2O_4 + InBO_3$
2	40	5	55	950	$Ca_2B_2O_5 + CaB_2O_4 + InBO_3$
3	33.3	22.2	44.5	1000	$T + Ca_2B_2O_5 + InBO_3$
4	50	5	45	950	$T + Ca_2B_2O_5 + Ca_3B_2O_6$
5	25	40	35	1200	$T + InBO_3 + In_2O_3$
6	30	45	25	1200	$Ca_3B_2O_6 + In_2O_3$
7	40	40	20	1200	$Ca_3B_2O_6 + In_2O_3 + CaIn_2O_4$
8	60	25	15	1000	$Ca_3B_2O_6 + CaO + CaIn_2O_4$
9	70	15	15	1200	$Ca_3B_2O_6 + CaO + CaIn_2O_4$
H	33.4	66.6	0	1350	$CaIn_2O_4$
T	33.3	33.3	33.4	1050	$T + In_2O_3$

spectrum was obtained at room temperature via a Perkin-Elmer 983G infrared spectrophotometer with KBr pellets as standards. It was collected in a range from 400 to 2000 cm^{-1} with a resolution of 1 cm^{-1}.

3. Results and discussion

3.1. Subsolidus phase relations in CaO–In_2O_3–B_2O_3 system

In the binary system CaO–B_2O_3, six binary compounds CaB_6O_{10} [11], CaB_4O_7 [12], CaB_2O_4 [ICDD-PDF 76-0747], $Ca_2B_2O_5$ [ICDD-PDF 79-1516], $Ca_3B_2O_6$ [13], and $Ca_2B_6O_{11}$ [14], have been reported. In the work of Hart and Brown [15], $Ca_2B_6O_{11}$ was synthesized under a hydrothermal condition. We did not observe CaB_4O_7. Yet, there is a possibility that CaB_4O_7 decomposes into CaB_6O_{10} and CaB_2O_4 above 800 °C. A detailed study of thermal stability of CaB_4O_7 will be necessary. The other four compounds were confirmed in our experiment.

In the system CaO–In_2O_3, two binary compounds have been reported, namely, $CaIn_2O_4$ [16], and $Ca_3In_2O_6$ [ICDD-PDF 73-0154]. According to the literature [17], Schenck and Müller-Buschbaum synthesized $Ca_3In_2O_6$ at above 2000 °C. So, only $CaIn_2O_4$ was obtained under our present work.

As for the binary system In_2O_3–B_2O_3, one binary compound $InBO_3$ was reported by [PDF 82-1188] and confirmed in our experiment.

Based on the phase identifications of eleven samples with different compositions as listed in Table 1, the subsolidus phase relations of CaO–In_2O_3–B_2O_3 system were determined under present experimental conditions, as shown in Fig. 1. There are 9 definite three-phase regions. No solid solution regions were observed in all binary and ternary compounds, and two-phase regions are all joint-lines of relevant two compounds. Ternary compound, $CaInBO_4$ was found and confirmed in this system. Comparing with our work, the powder XRD pattern [9] reported in ICDD-PDF 27-1055 was found incomplete. Moreover, the crystal structure of this compound has no report in previous literatures. Thus, we reinvestigated the crystal structure of compound $CaInBO_4$, which will be discussed in the following section.

3.2. Crystal structure of $CaInBO_4$

Using the program DICVOL04 [18] by successive dichotomy method with Si as the internal standard, all the reflections ($2\theta \leq 50°$) of the compound $CaInBO_4$ can be well indexed on the basis of an orthorhombic unit cell with lattice parameters $a = 10.3134(9)$ Å, $b = 9.5159(7)$, and $c = 3.4243(1)$ Å. Reflection conditions with $0\,k\,l$: $k + l = 2n$, $h\,k\,0$: $h = 2n$, $h\,0\,0$: $h = 2n$, $0\,k\,0$: $k = 2n$, and $0\,0\,l$: $l = 2n$ are consistent with space group $Pn2_1a$ and Pnma. Comparisons between $CaInBO_4$ and $CaYBO_4$ in crystal system, lattice parameters and powder XRD pattern show that the two compounds may be isostructural. So we choose the space group Pnma.

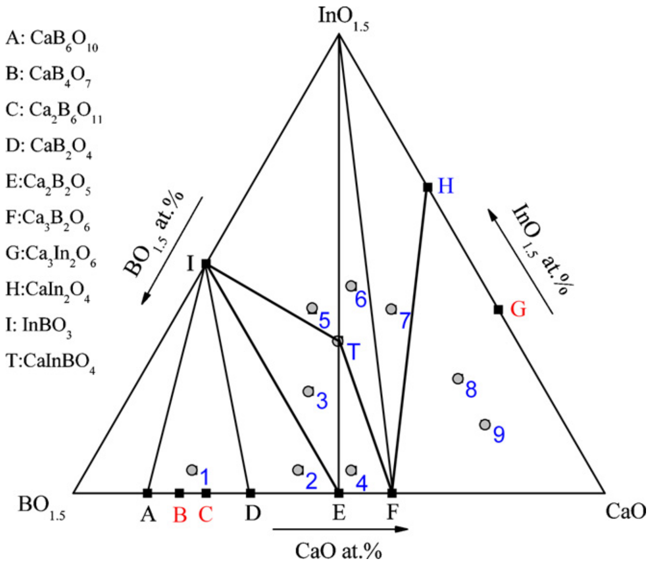

Fig. 1. Subsolidus phase relations in the system CaO–In_2O_3–B_2O_3.

In addition, there is no efficiency of second harmonic generation (SHG) in powder samples of $CaInBO_4$ using the Kurtz–Perry technique [19], which suggests centrosymmetric Pnma space group is more probable.

Taking $CaYBO_4$ as the preliminary crystal structural model, we refined the structure parameters of $CaInBO_4$ from the powder XRD data by the Rietveld method [20] using the program FullProf_suite [21]. The profile range of data used for structure refinement is 10–130° in 2θ, and the Pseudo-Voigt function was used as peak shape function. A total of 42 parameters were refined in the refinement, including background parameters, profile parameters, and structural parameters. As for atomic coordinates, all atoms are located on the crystal lattice position 4*c* similar to the case for $CaYBO_4$ [10]. The agreement factors in the structural refinement finally were converged to $R_B = 4.56\%$, $R_P = 7.37\%$, $R_{WP} = 10.9\%$ and $S = 2.67$, which indicates the structure model is quite right. Fig. 2 shows the final refinement pattern. Details of Rietveld refinement and crystal data are given in Table 2. Positional parameters obtained by the Rietveld refinement are listed in Table 3. By the way, we have

Table 2
Details of Rietveld refinement and crystal data for the structure $CaInBO_4$.

Sample	Multi-crystal powder
Diffractometer	Rigaku D/MAX-2500
Radiation type	Cu Kα
Monochromator	Graphite
Wavelength (Å)	1.5405
Refined profile range (°2θ)	10–130
Step size (°2θ)	0.02
Step scan time per step (s)	2
Number of structure parameters	29
Number of profile parameters	13
R_B	4.56%
R_P	7.37%
R_{WP}	10.9%
S	2.67
Formula	$CaInBO_4$
Symmetry	Orthorhombic
Space group	Pnma
a (Å)	10.3120(3)
b (Å)	3.42519(8)
c (Å)	9.3950(3)
Volume (Å^3)	336.07(2)
Z	4
Calculated density (g cm^{-3})	2.73

Table 3
Atomic coordinates and isotropic displacement parameters for $CaInBO_4$.

Atom	Site	x	y	z	B (Å^2)	Occ.
Ca1	4c	0.0879(3)	0.25	0.6563(3)	1.25(1)	0.936
In1	4c	0.0879(3)	0.25	0.6563(3)	1.25(1)	0.064
In2	4c	0.1132(1)	0.25	0.0701(1)	0.313(6)	0.936
Ca2	4c	0.1132(1)	0.25	0.0701(1)	0.313(6)	0.064
O1	4c	0.2514(9)	0.25	0.2385(9)	0.56(4)	1
O2	4c	0.2579(8)	0.25	0.4883(9)	0.24(4)	1
O3	4c	0.5089(8)	0.25	0.6251(9)	0.71(3)	1
O4	4c	0.0547(8)	0.25	0.3821(9)	0.13(1)	1
B1	4c	0.1867(8)	0.25	0.3682(9)	0.90(1)	1

refined the Ca/In mixed occupation ratios of the two 4c sites, but the results are unreasonable. Compared to the presented mixed occupation, the agreement factors were worse when we refined the structure without a mixed occupation of these 4c sites. So we kept the Ca/In mixed occupation ratios of the model $CaYBO_4$.

Fig. 3 shows crystal structural projection of $CaInBO_4$ along the [0 1 0] direction. The $CaInBO_4$ orthorhombic cell results from the condensation of distorted Ca(1)/In(1)O_7 polyhedra, In(2)/Ca(2)O_6 octahedra and trigonal BO_3 groups. The planar BO_3 trigons are parallel to each other and stack layer upon layer along the b axis. The Ca(1)/In(1)O_7 polyhedra connect each other by sharing their edges and forming $[Ca(1)/In(1)]_2O_{12}$, which give nearly linear double-chains and infinitely extend along the b axis. For $[In(2)/Ca(2)]_2O_{10}$ double-chains along the b axis, the situation is similar. Linkages of different chains in the cell are ensured by sharing edges and vertices with BO_3 groups. The connections of In(2)/Ca(2)O_6 octahedra, Ca(1)/In(1)O_7 polyhedra and BO_3 groups are depicted in Figs. 4 and 5, respectively.

In the building units of $CaInBO_4$ structure, the B—O bond lengths vary from 1.36(1) to 1.40(1) Å with an average value of 1.38 Å, and the O—B—O angles are between 117.1(6) and 123.9(6)°. These values are normal in a BO_3 plane triangle. The Ca(1)/In(1) atom is bound to seven O atoms at length ranging from 2.234(9) to 2.631(9) Å with average Ca(1)/In(1)—O distance, 2.404 Å, which agrees well with the average Ca—O value 2.419 Å reported in $LiCaBO_3$ [22]. The oxygen polyhedron of one independent In(2)/Ca(2) site is a regular In(2)/Ca(2)O_6 octahedron with In(2)/Ca(2)—O distances between 2.144(9) and 2.303(5) Å. The average In(2)/Ca(2)—O distance, 2.212 Å, is longer than the value 2.18 Å for In—O bond length in $Ba_3InB_9O_{18}$ [23]. These results may be ascribed to the mixed occupancies between Ca and In atoms in the structure of $CaInBO_4$.

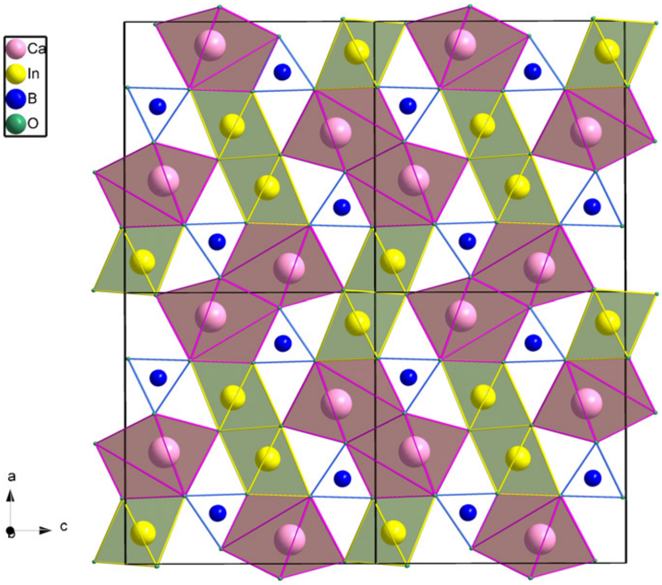

Fig. 3. Crystal structure of $CaInBO_4$ along the [0 1 0] direction. Large gray circles stand for Ca(1)/In(1) atoms, small gray circles for In(2)/Ca(2) atoms, big black circles for B atoms, small black circles for O atoms (in black-and-white for printing purpose).

All standard deviations for bond lengths and angles are within experimental error expected for metrically regular geometries. Some selected geometric parameters in the structure of $CaInBO_4$ are listed in Table 4. To examine the validity of the determined structure of $CaInBO_4$, Brown's bond valence method [24] was used to calculate the valence sum for each ion. From the results given in Table 5, it is proposed that the calculated valence sums for all ions are reasonable considering the situation of mixed occupancies in this structure.

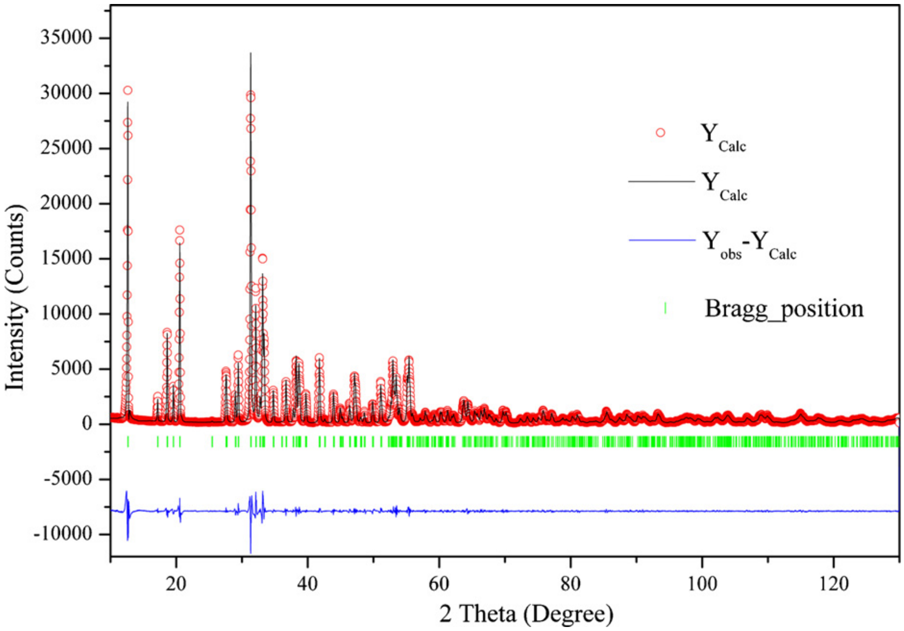

Fig. 2. Final Rietveld refinement patterns for $CaInBO_4$. Small dots represent the experimental values and solid lines for the calculated pattern. The solid line at the bottom is the difference between the experimental and calculated values. The vertical bars show the positions of the calculated Bragg reflections.

Table 4
Selected geometric parameters (Å or°) in structure $CaInBO_4$.

Ca(1)/In(1)	—O(3)[a]	2.234(9) (Å)	In(2)/Ca(2)	—O(1)	2.144(9) (Å)
	—O(4)[b]	2.287(6) (Å)		—O(3)[f]	2.146(8) (Å)
	—O(4)[c]	2.287(6) (Å)		—O(3)[g]	2.189(5) (Å)
	—O(2)	2.372(9) (Å)		—O(3)[h]	2.189(5) (Å)
	—O(1)[d]	2.508(7) (Å)		—O(2)[h]	2.303(5) (Å)
	—O(1)[e]	2.508(7) (Å)		—O(2)[i]	2.303(5) (Å)
	—O(4)	2.631(9) (Å)			
B(1)	—O(2)	1.36(1) (Å)	O(2)—B(1)—O(4)	117.1(6) (°)	
	—O(4)	1.37(1) (Å)	O(2)—B(1)—O(1)	118.8(6) (°)	
	—O(1)	1.40(1) (Å)	O(2)—B(1)—O(1)	123.9(6) (°)	

[a] $-1/2+x, 1/2-y, 3/2-z$.
[b] $-x, 1/2+y, 1-z$.
[c] $-x, -1/2+y, 1-z$.
[d] $1/2-x, 1-y, 1/2+z$.
[e] $1/2-x, -y, 1/2+z$.
[f] $-1/2+x, 1/2-y, 1/2-z$.
[g] $1/2-x, -y, -1/2+z$.
[h] $1/2-x, 1-y, -1/2+z$.
[i] $1/2-x, -y, -1/2+z$.

Table 5
Bond valence analysis of $CaInBO_4$.

Atoms	O(1)	O(2)	O(3)	O(4)	Σs_{calc}	Σs_{theo}
Ca(1)/In(1)	0.2317*2	0.3347*1	0.4860*1	0.4211*20.1662*1	2.2925	2.064
In(2)/Ca(2)	0.5199*1	0.3383*2	0.5171*10.4604*2		2.6344	2.936
B(1)	0.925*1	1.0271*1		0.9995*1	2.9516	3
Σs_{calc}	1.9083	2.0384	1.9239	2.0079		
Σs_{theo}	2	2	2	2		

Note. The results refer to the equation $s = \exp[(r_0 - r)/B]$ with r_0 = 1.967 Å, 1.902 Å and 1.371 Å for Ca—O, In—O and B—O, respectively, and B = 0.37.

3.3. *IR spectra*

In order to further confirm the coordination surroundings of B—O in the $CaInBO_4$ structure, an infrared absorption spectrum for $CaInBO_4$ was measured at room temperature and given in Fig. 6. Bands below 500 cm^{-1} mainly originates from the lattice dynamic modes, while the absorption wavenumber profile in 600–800 cm^{-1} is assigned to plane bending vibration of BO_3 units. According to Kamitsos's report [25], the strong absorption wavenumber profile above 1145 cm^{-1} are generated by the stretching vibrations of the triangular BO_3 groups. It is found that there are several closely spaced peaks about 1200 cm^{-1}, which are believed to come from the different bond lengths of B—O.

In crystal structure of this complex borate, the boron atoms are trigonally coordinated by oxygen atoms, which is confirmed by the appearance of characteristic frequencies of an isolated plane triangle of symmetry in the spectral region studied. The infrared absorption spectra of compound $CaInBO_4$ indicates that its crystal structure is agree with the X-ray powder diffraction data, confirming the existence of the $[BO_3]^{3-}$ groups. This result is similar to what were reported in previous works [25,26].

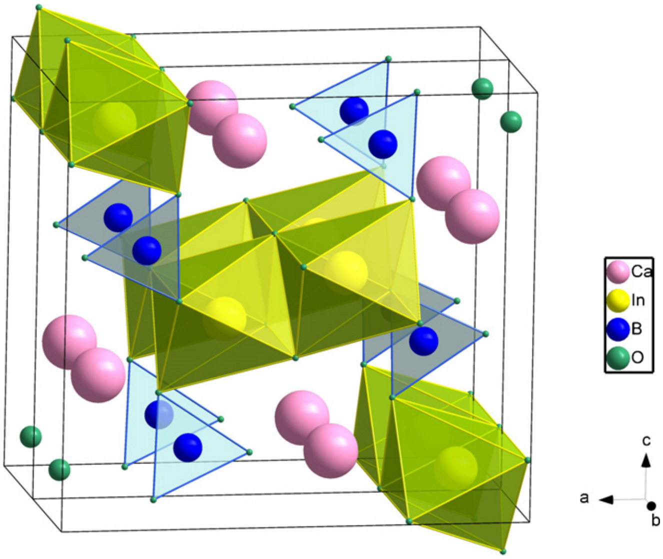

Fig. 4. View of the connection between $In(2)/Ca(2)O_6$ octahedra and triangular BO_3 groups.

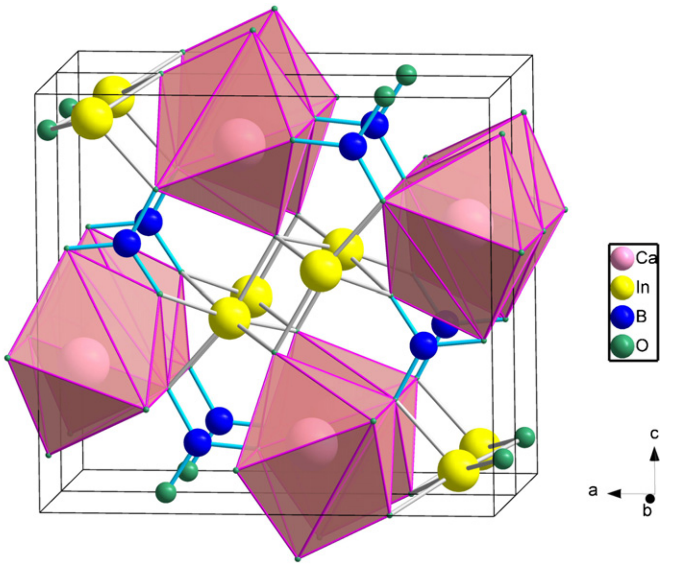

Fig. 5. The connection of distorted $Ca(1)/In(1)O_7$ polyhedra and triangular BO_3 groups.

Table 6
Crystal information of compounds $MRBO_4$ (M and R are divalent and trivalent cations, respectively).

Compound	R^{3+}/M^{2+}	S.G.	a (Å)	b (Å)	c (Å)	V (Å^3)	Z
$MgAlBO_4$ [27]	0.7727	Pnma(62)	9.8780	5.6750	4.3280	242.62	4
$MgGaBO_4$ [28]	0.9394	Pnma(62)	9.1847	3.0779	9.2942	262.74	4
$MgScBO_4$ [29]	1.1061	Pnma(62)	9.4900	3.2189	9.4420	288.43	4
$ZnFeBO_4$ [30]	0.8649	Pnma(62)	9.2462	3.1410	9.3530	271.63	4
$CaAlBO_4$ [31]	0.5152	Ccc2(37)	8.2690	15.2270	5.7330	721.85	8
$CaGaBO_4$ [32]	0.6263	Ccc2(37)	8.2940	15.4730	5.8392	749.36	8
$CaInBO_4$ [a]	0.8182	Pnma(62)	10.3120	3.4252	9.3950	336.07	4
$CaYBO_4$ [10]	0.8990	Pnma(62)	10.4354	3.5880	9.6126	359.92	4
$SrAlBO_4$ [33]	0.4554	Pccn(56)	8.8600	15.1700	5.4800	736.55	8
β-$SrGaBO_4$ [34]	0.5536	$P2_12_12$(18)	8.9921	15.3707	5.9191	818.11	8
α-$SrGaBO_4$ [35]	0.5536	Pccn(56)	8.9186	15.3154	5.8130	794.01	8
$PbAlBO_4$ [36]	0.425	Pnma(62)	6.9209	5.7134	8.0215	317.19	4
$PbCrBO_4$ [37]	0.525	Pnma(62)	6.9501	5.9410	8.1386	336.05	4
$PbGaBO_4$ [38]	0.5167	Pnma(62)	6.9944	5.8925	8.2495	340	4
$PbFeBO_4$ [37]	0.5333	Pnma(62)	7.0089	5.9412	8.3339	347.03	4
$PbBiBO_4$ [39]	0.8	$P12_1/c1$(14)	7.4730	7.5170	10.5264	427.29	4
$BaBiBO_4$ [40]	0.7164	$Pna2_1$(33)	8.5817	9.6802	5.1505	427.87	4

[a] This work.

3.4. *Crystal structure of compounds $MRBO_4$ (M and R are divalent and trivalent cations, respectively) [27–40]*

Although the title compound has the similar isolated planar $[BO_3]^{3-}$ anionic groups and the same formula $MRBO_4$ with $CaAlBO_4$, $SrGaBO_4$, $PbBiBO_4$ and $BaBiBO_4$, different structures are found in those borates. The structure types strictly depend on the relative size of the two cations of these compounds. Table 6 lists crystal informations of compounds $MRBO_4$ (M = Mg, Zn, Ca, Sr, Pb, Ba; R = Al, Ga, Cr, Fe, Sc, In, Y, Bi) reported in both previous literatures and this work. From Table 6, one can see that unit cell with the Pnma type expands linearly with the increasing of M′ and R′ ionic radius. Most is worth mentioning, values for R^{3+}/M^{2+} in $MRBO_4$ are between 0.425 for $PbAlBO_4$ up to 1.1061 for $MgScBO_4$, as shown in Fig. 7. Both $CaGaBO_4$ structure and $BaBiBO_4$ structure have lower-symmetry, which the values for R^{3+}/M^{2+} in these crystal structures are in the range from 0.6 to 0.7. Obviously, the symmetry of Bi derivatives are much lower and decreases with the reduction of M′ ionic radius. In authors' opinion, there are still many possible derivatives of $MRBO_4$ if the R^{3+}/M^{2+} ratios are dominant in determining stability of these structures. The possible derivatives may include $ZnAlBO_4$, $ZnGaBO_4$, $ZnScBO_4$, $ZnInBO_4$, $MgInBO_4$, $PbScBO_4$, $PbInBO_4$ and so on. Of course, the existences of those derivatives need to be confirmed by experiments. From the point of rule for ionic radii ratios, there must exist upper and lower limit for R^{3+}/M^{2+} in those compounds. In order to determine the maximum and minimum of R^{3+}/M^{2+} values and the relation to symmetry of $MRBO_4$, syntheses of other substituted derivatives remain to be investigated in the future work.

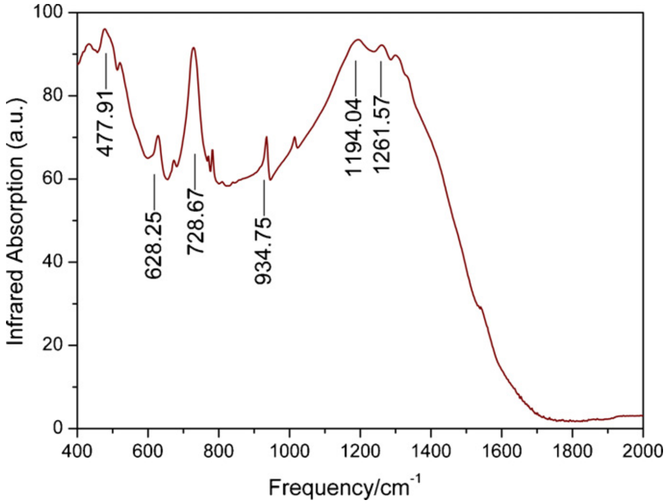

Fig. 6. Infrared spectra for powder $CaInBO_4$ sample.

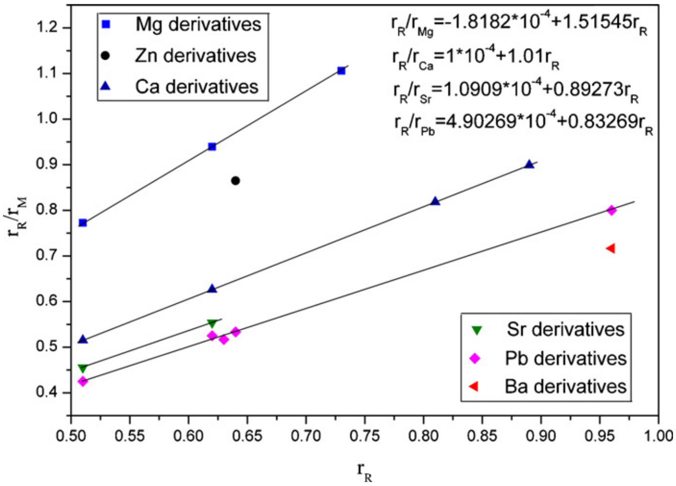

Fig. 7. The evolution of the ionic radii ratios M/R with increasing R^{3+} radius for $MRBO_4$ (M and R are divalent and trivalent cations, respectively) compounds.

4. Conclusions

In this work, the subsolidus phase relations of $CaO–In_2O_3–B_2O_3$ system were established. The crystal structure of ternary compound $CaInBO_4$ in this system was determined from powder X-ray diffraction data using Rietveld method. It has a stacked structure consisting of $Ca(1)/In(1)O_7$ polyhedra and $In(2)/Ca(2)O_6$ octahedra connected each other sharing vertices and edges of BO_3 groups, with the nearly linear $—[Ca(1)/In(1)]_2O_{12}—$ double-chains and $—[In(2)/Ca(2)]_2O_{10}—$ double-chains extending infinitely along the *b* axis. $CaInBO_4$ is isostructural to $CaYBO_4$, with the similar chemical bond nature around metal cations. Coordination surrounding of B—O in this structure, $[BO_3]^{3-}$ group, was confirmed by infrared absorption spectrum of $CaInBO_4$. The planar BO_3 trigons are parallel to each other and stack layer upon layer along the *b* axis. A large birefringence is expected from this structural character for $[BO_3]^{3-}$ group. The compounds with the $MRBO_4$ formula (M = divalent cations, R = trivalent cations) are in a large family of monoborates with different structure types strictly depending on the relative size of the M and R ions. The variety of the $MRBO_4$

structures may be of benefit to tailoring the physical and chemical properties of these materials.

Acknowledgements

Financial support by the National Natural Science Foundation of China (Grant number 51002189.) is gratefully acknowledged. The work was also supported through a Grant-in-Aid from Department for Science and Technology of Hunan province. The authors thank Hong Bo, and Jiwu Huang (School of Materials Science and Engineering, Central South University, Changsha, Hunan 410083, PR China) for their kind help.

References

[1] P.D. Thompson, J.F. Huang, R.W. Smith, D.A. Keszler, J. Solid State Chem. 95 (1991) 126.
[2] M. He, L. Kienle, A. Simon, X.L. Chen, V. Duppel, J. Solid State Chem. 177 (2004) 3212.
[3] P. Gravereau, J.P. Chaminade, S. Pechev, V. Nikolov, D. Ivanova, P. Peshev, Solid State Sci. 4 (2002) 993.
[4] Z.G. Hu, T. Higashiyama, M. Yoshimura, Y.K. Yap, Y. Mori, T. Sasaki, Jpn. J. Appl. Phys. 37 (1998) L1093.
[5] L. He, Y.H. Wang, J. Alloys Compd. 431 (2007) 226.
[6] V. Jubera, J.P. Chaminade, A. Garcia, F. Guillen, C. Fouassier, J. Lumin. 101 (2003) 1.
[7] G.M. Cai, F. Zheng, D.Q. Yi, Z.P. Jin, X.L. Chen, J. Lumin. 130 (2010) 910.
[8] G. Blasse, J. Inorg. Nucl. Chem. 31 (1969) 1519.
[9] J.J. Capponi, J.##E.T. Chenavas, J.C. Joubert, J. Solid State Chem. 7 (1973) 49.
[10] Y. Zhang, X.L. Chen, J.K. Liang, T. Xu, Y.P. Xu, J. Alloys Compd. 327 (2001) 132.
[11] X.A. Chen, M. Li, X.N. Chang, H.G. Zang, W.Q. Xiao, J. Alloys Compd. 464 (2008) 332.
[12] N.V. Zarakina, A.A. Brovkin, Kristallografiya 22 (1977) 275.
[13] A. Vegas, F.H. Cano, S. García-Blanco, Acta Crystallogr. B 31 (1975) 1416.
[14] N.V. Zarakina, A.A. Brovkin, Kristallografiya 21 (1976) 502.
[15] P.B. Hart, C.S. Brown, J. Inorg. Nucl. Chem. 24 (1962) 1057.
[16] L. Passerini, Gazz. Chim. Ital. 60 (1930) 754.
[17] R.V. Schenck, H. Müller-Buschbaum, Z. Anorg. Allg. Chem. 398 (1973) 15.
[18] A. Boultif, D. Louer, J. Appl. Crystallogr. 37 (2004) 724.
[19] A. Akella, D.A. Keszler, J. Solid State Chem. 120 (1995) 74.
[20] H.M. Rietveld, Acta Crystallogr. 22 (1967) 151.
[21] J. Rodriguez-Carvajal, FullProf (Version 3.5d Oct98-LLB-JRC).
[22] L. Wu, X.L. Chen, H. Li, M. He, L. Dai, X.Z. Li, Y.P. Xu, J. Solid State Chem. 177 (2004) 1111.
[23] G.M. Cai, X.L. Chen, W.Y. Wang, Y.F. Lou, J. Liu, J.T. Zhao, H.H. Chen, J. Solid State Chem. 181 (2008) 646.
[24] I.D. Brown, D. Altermatt, Acta Crystallogr. B 41 (1985) 244.
[25] E.I. Kamitsos, M. Karakassides, G.D. Chryssikos, J. Phys. Chem. 91 (1987) 1073.
[26] G.M. Cai, Y. Sun, H.K. Li, X. Fan, X.L. Chen, F. Zheng, Z.P. Jin, Mater. Chem. Phys. 129 (2011) 761.
[27] J.H. Fang, R.E. Newnham, Mineral. Mag. J. Mineral. Soc. (1876–1968) 35 (1965) 196.
[28] Z. Yang, X.L. Chen, J.K. Liang, Y.C. Lan, T. Xu, J. Alloys Compd. 319 (2001) 247.
[29] R. Norrestam, Z. Kristallogr. 189 (1989) 1.
[30] S. Busche, K. Bluhm, Z. Naturforsch, B. Anorg, Chem. Org. Chem. 50 (1995) 1450.
[31] W. Schuckmann, Neues Jahrb. Mineral., Monatsh. 1968 (1968) 80.
[32] Z. Yang, J.K. Liang, X.L. Chen, T. Xu, Y.P. Xu, J. Alloys Compd. 327 (2001) 215.
[33] T. Nagai, M. Ihara, J. Ceram. Assoc., Jpn. 80 (1972) 432.
[34] Z. Yang, J.K. Liang, X.L. Chen, J.R. Chen, J. Solid State Chem. 165 (2002) 119.
[35] Z. Yang, X.L. Chen, J.K. Liang, M. He, J.R. Chen, Cryst. Res. Technol. 39 (2004) 634.
[36] H.-S. Park, J. Barbier, R.P. Hammond, Solid State Sci. 5 (2003) 565.
[37] H. Park, R. Lam, J.E. Greedan, J. Barbier, Chem. Mater. 15 (2003) 1703.
[38] H. Park, J. Barbier, Acta Crystallogr., Sect. E: Struct. Rep. Online 57 (2001) 82.
[39] X. Chen, J. Zuo, X. Chang, Y. Zhao, H. Zang, W. Xiao, J. Solid State Chem. 179 (2006) 3191.
[40] J. Barbier, N. Penin, A. Denoyer, L.M.D. Cranswick, Solid State Sci. 7 (2005) 1055.